

**Photoluminescence of bulk germanium**R. R. Lieten,<sup>1,2,3,\*</sup> K. Bustillo,<sup>4</sup> T. Smets,<sup>1</sup> E. Simoen,<sup>3</sup> J. W. Ager III,<sup>2</sup> E. E. Haller,<sup>2,4</sup> and J.-P. Locquet<sup>1</sup><sup>1</sup>*Department of Physics and Astronomy, K.U. Leuven, 3001 Leuven, Belgium*<sup>2</sup>*Division of Materials Sciences, Lawrence Berkeley National Laboratory, Berkeley, California 94720, USA*<sup>3</sup>*IMEC, 3001 Leuven, Belgium*<sup>4</sup>*Department of Materials Science and Engineering, University of California, Berkeley, California 94720, USA*

(Received 25 April 2012; published 9 July 2012)

We have performed photoluminescence (PL) measurements on intrinsic and doped bulk Ge substrates as a function of temperature and excitation power. A weak luminescence feature at 738 meV is observed at 7 K for Ge substrates with Al and Sb dopants, but not for intrinsic and Ga-doped Ge. This feature can be explained by no-phonon (NP)-assisted recombination of free excitons. Besides the NP feature, we observe intense luminescence peaks at 730, 710, and 702 meV, which can be attributed to phonon-assisted exciton recombination of transverse acoustic (TA), longitudinal acoustic (LA), and transverse optical (TO) phonons in the (111) direction, respectively. Besides these features, we observe luminescence at energy below 700 meV (1.77  $\mu\text{m}$ ). This luminescence shows much lower intensity (about 500 times) than the LA replica. The observed luminescence can be explained as a two-phonon-assisted recombination with the previously mentioned TA, LA, and TO phonons with momentum in the (111) direction (at the  $L$  point) and a TO phonon at the  $\Gamma$  point. The power dependence of the integrated PL shows a log-log dependence with power factor of 2.02 at 9 K. This confirms that the PL originates from recombination of excitons, which are indirectly generated by creation of electrons and holes. The low-energy PL edge follows the temperature dependence of the band gap as a function of temperature, whereas the high-energy PL edge shows an exponential broadening as a function of temperature.

DOI: [10.1103/PhysRevB.86.035204](https://doi.org/10.1103/PhysRevB.86.035204)

PACS number(s): 78.55.-m

**I. INTRODUCTION**

Germanium has, besides high carrier mobilities, interesting optical properties. Ge absorbs infrared light efficiently compared to silicon. The absorption depth of light with a wavelength of 850 nm (1.46 eV) decreases from 17  $\mu\text{m}$  in Si to 0.3  $\mu\text{m}$  in Ge.<sup>1</sup> Introduction of tensile strain can be used to improve the light emission of Ge.<sup>2</sup> Recently Ge has received a lot of attention for its use in photodetectors, integrated on Si.<sup>3-7</sup> Furthermore optically pumped lasing<sup>8</sup> and electrically pumped lasing<sup>9</sup> in Ge, integrated on Si substrates, have been demonstrated very recently. Thin Ge layers on Si substrates can therefore be used to integrate fast Ge photodetectors and modulators on Si complementary metal-oxide-semiconductor (CMOS) devices for optical interconnects.

In view of this renewed interest in the optical properties of Ge, we have performed photoluminescence (PL) measurements on intrinsic and doped Ge substrates as a function of temperature and excitation power. PL measurements are very well suited for the study of radiative recombination mechanisms of excess carriers in Ge and holds information on the nature and occurrence of radiative transitions, the presence of crystal defects, impurities, and dopants.

**II. EXPERIMENT**

Bulk Ge substrates, fabricated at the Lawrence Berkeley National Lab and Umicore, were used for this work. These substrates were grown by the Czochralski method.<sup>10,11</sup> The presence of dopants in the melt influences the formation of crystal defects during the pulling process.<sup>10</sup> For this reason it is interesting to look at the influence of dopants on the photoluminescence spectra. Doped substrates were obtained by introducing Sb, Al, and Ga dopants with levels of

(1–6)  $\times 10^{16}$   $\text{cm}^{-3}$ . In addition to substrates with dopants, intrinsic substrates were fabricated with a carrier concentration of  $3 \times 10^{11}$   $\text{cm}^{-3}$ . PL measurements were performed in the backscattering geometry using a SPEX 1680 0.22-m double spectrometer and InGaAs photodiode detector cooled to 77 K. The InGaAs detector and spectrometer allow the measurement of photons with energy down to 0.566 eV (2190 nm). PL spectra were corrected for the instrument response using a black-body calibration lamp. An argon laser source with wavelength of 514 nm (2.41 eV) was used as excitation source, and a maximum excitation power of 128  $\text{W}/\text{cm}^2$ . Samples were cooled to 19 K using a closed-cycle cryostat and to 4.3 K using a continuous-flow He cryostat.

**III. PL PEAK ASSIGNMENTS**

Photoluminescence spectra of intrinsic, Al-doped, Ga-doped, and Sb-doped bulk Ge at 7 K are shown in Fig. 1. A weak luminescence feature at 738 meV is observed at 7 K for Ge substrates with Al and Sb dopants. This feature can be explained by no-phonon (NP)-assisted recombination of free excitons. The impurity levels in the intrinsic substrate are too low to observe NP-assisted recombination. In the case of Ga doping the NP-assisted recombination cannot be observed because Ga has almost the same size as Ge and will not induce sufficient vibrations. At 7 K, the indirect band-gap energy and free exciton binding energy of Ge are 742 and 4.2 meV, respectively.<sup>12,13</sup> Besides the NP feature for doped germanium, we observe intense luminescence peaks at 730, 710, and 702 meV in all samples, which can be attributed to phonon-assisted exciton recombination of transverse acoustic (TA), longitudinal acoustic (LA) and transverse optical (TO) phonons in the (111) direction; see Table I.<sup>14</sup> These phonons

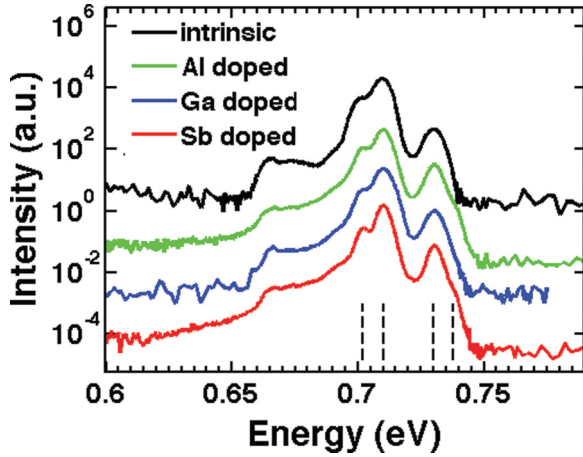


FIG. 1. (Color online) Photoluminescence measurement at 7 K of intrinsic, Al-doped, Ga-doped, and Sb-doped bulk Ge. Similar features are observed, independently of the presence of dopants. The substrates with Al and Sb dopants show an additional NP peak.

are emitted to conserve the momentum for the indirect transition of electrons to the valence band.<sup>15</sup> The one-phonon-assisted peaks are shifted from the band-gap energy by the sum of the phonon energy and the exciton energy towards lower energies. With the exception of the 738-meV NP peak, the PL line shape of intrinsic Ge appears unchanged by the addition of Al, Ga, and Sb dopants at concentrations of  $(1-6) \times 10^{16} \text{ cm}^{-3}$ . Defects induced during the crystal growth due to dopant addition do not have an effect on the measured line shape. Although it has been suggested that the TA and longitudinal optical (LO) phonon-assisted transitions are forbidden at the  $L$  point in Ge, allowed transitions are possible if electrons and holes are in the vicinity.<sup>16</sup> These data demonstrate that LA, TO, and TA one-phonon-assisted transitions are present in the intrinsic and doped material. Because the LO phonon has energy close to the LA phonon in the (111) direction, the LO phonon-assisted transition could not be resolved at 4.3 K.

Besides the one-phonon features, we observe luminescence at energy below 700 meV ( $1.77 \mu\text{m}$ ), as shown in Fig. 2. This luminescence shows much lower intensity (about 500 times) than the LA replica. We explain the observed luminescence as a two-phonon-assisted recombination with the previously mentioned TA, LA (LO), and TO phonons with momentum in the (111) direction (at the  $L$  point) and a TO phonon at the  $\Gamma$  point. Figure 2 shows the peak assignments for Al-doped Ge at 4.3 K. The phonons at the  $L$  point give the required momentum transfer whereas the TO phonon at the  $\Gamma$  point

TABLE I. Phonon energies at  $L$  valley and corresponding exciton replica energy at 4.3 K. (Ref. 14).

	Energy ( $L$ ) (meV)	Exciton replica (4.3 K)
TA	8	730
LA	28	710
LO	30	708
TO	36	702

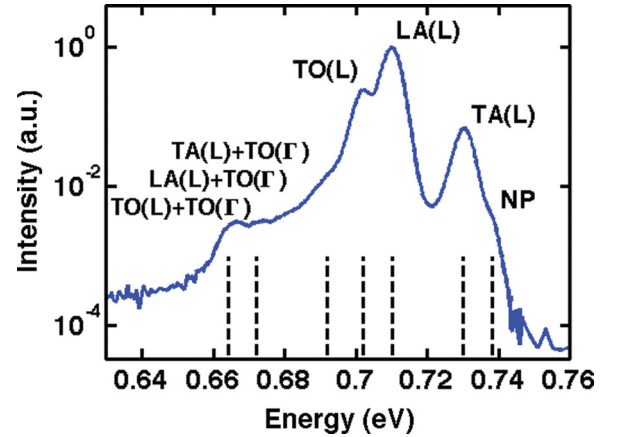


FIG. 2. (Color online) Photoluminescence measurement of Al-doped Ge at 4.3 K shows PL at energy below 700 meV ( $1.77 \mu\text{m}$ ).

lowers the transition energy with 38 meV and does not change the momentum.

We did not observe luminescence from the direct transition [0.89 eV at 4.3 K (Ref. 12)]. Direct gap luminescence can be obtained by using high excitation densities,<sup>17</sup> high dopant concentrations,<sup>18</sup> or strain.<sup>19</sup>

#### IV. POWER DEPENDENCE

The power dependence of the near-band-edge photoluminescence of semiconductors holds information on the nature of the transition.<sup>20</sup> In general the PL intensity  $I_{\text{PL}}$  is proportional to  $(I_{\text{excitation}})^b$ ;  $I_{\text{excitation}}$  is the intensity of the excitation laser power. The power factor  $b$  is in between 1 and 2 for excitonlike transitions. For free-to-bound and donor-acceptor pair transitions  $b < 1$ .<sup>20</sup> In the case of direct generation of excitons from the excitation source,  $b$  equals 1.<sup>20</sup> In the case of the direct band-gap semiconductor CdTe a factor of 1.25 has been measured for the free exciton recombination.<sup>21</sup> We have performed power-dependent PL measurements on Sb-doped Ge substrates at 9 K; see Fig. 3(a). A log-log plot of the integrated PL signal as function of excitation power shows a clear linear dependence; see Fig. 3(b). The data were fitted by the equation  $I_{\text{PL}} = a(I_{\text{excitation}})^b$ . For the power factor  $b$ , we obtained a value of 2.02. This indicates that the PL originates from the recombination of excitons. Furthermore the quadratic dependence shows that these excitons are indirectly generated from photogenerated electrons and holes and that only a minor part of these photogenerated carriers form excitons at the applied excitation density. Most electrons and holes recombine nonradiatively via defect states. We also looked at the power dependence of the maximum intensity of the LA phonon replica, TA phonon replica, and the second-order TO( $L$ ) + TO( $\Gamma$ ) phonon replica. For the LA and TA phonon replica, as well as the second-order TO( $L$ ) + TO( $\Gamma$ ) phonon replica, we observe quadratic power dependence. We have used relatively small laser powers ( $\leq 128 \text{ W/cm}^2$ ) and therefore we do not observe a Burstein-Moss (blue) shift towards the direct band-gap transition,<sup>22</sup> except for a small Burstein-Moss shift of 2 meV at  $128 \text{ W/cm}^2$  power density. We observe a different power dependence than Klingenstein and Schweizer,<sup>17</sup> who show a power factor of 1 for the indirect transition and 1.6 for

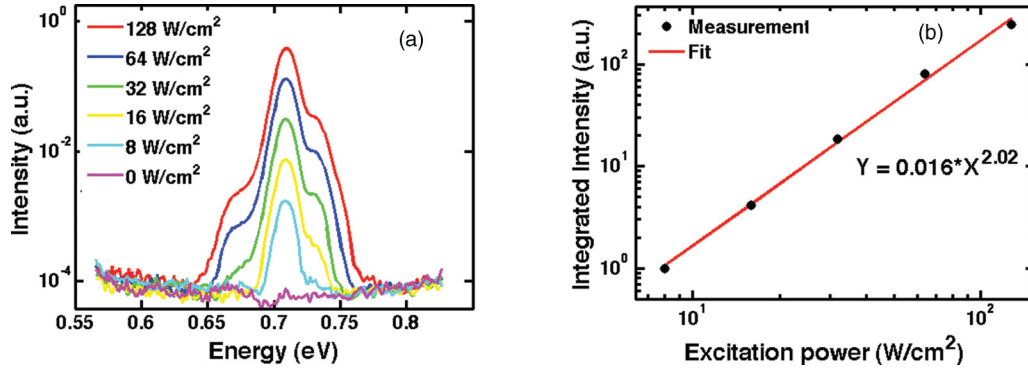


FIG. 3. (Color online) (a) Photoluminescence measurements at 9 K of Sb-doped Ge at different excitation powers. (b) Plot of integrated intensity as a function of excitation power. The integrated intensity shows quadratic dependence on excitation power. The maximum intensity of the TA, LA phonon replicas and second-order TO + TO phonon replica also show quadratic dependence.

the direct transition. This difference can be explained by the much higher excitation densities that were used by Klingenstein and Schweizer, which led to much larger electron and hole densities and even filling of the  $\Gamma$  valley. PL from the direct transition becomes visible and Auger recombination becomes more important, which will lead to smaller values for  $b$ .<sup>17</sup> Furthermore at high excitation densities an increase in excitation power will increase the density and recombination of excitons more than nonradiative recombination via defect states and will therefore lead to a reduction of the power factor  $b$ .

V. TEMPERATURE DEPENDENCE

Temperature-dependent PL measurements were performed on intrinsic Ge and are shown in Fig. 4(a). The PL spectrum becomes broader and the peak intensity decreases for increasing temperature. The left edge of the PL spectrum shows a clear red shift for increasing temperature. The energy of the left PL edge is plotted as function of temperature  $T$  in Fig. 4(b). The temperature dependence of the band-gap energy  $E_g$  of Ge can be described by Varshni’s empirical expression:  $E_g(T) = 0.742 - 4.8 \times 10^{-4} T^2 / (T + 235)$ .<sup>12</sup> At temperatures above 100 K the position of the left PL edge follows the band-gap temperature dependence, indicating this red shift originates from the band-gap shrinkage. At temperatures below 100 K

the temperature dependence shows an offset of 28 meV. This can be explained by a change in the phonon-assisted transition that determines the left PL edge: The TO phonon replica determines the left edge at temperatures below 100 K as is observed at low temperatures (when ignoring the much weaker two-phonon replicas); see Fig. 2. At temperatures above 100 K the left PL edge is determined by another transition with an increase in optical emission energy of 28 meV. This energy shift could be due to the dominance of the TA phonon emission, which is shifted by 28 meV in respect to the TO emission, or due to additional absorption of LA phonons at the  $L$  point. The right edge of the PL spectra shows a decreasing slope as a function of increasing temperature; see Fig. 4(a). The free excitons’ annihilation luminescence depends on the density of states and the probability function of excitons. The probability function of excitons follows the Fermi-Dirac probability function, which in the Boltzmann approximation becomes  $e^{-(E-E_0)/kT}$  with  $E_0 = E_g - E_{\text{exciton}} \pm E_{\text{phonon}}$ , where  $E_{\text{exciton}}$  is the free exciton binding energy and  $E_{\text{phonon}}$  is the phonon energy. For phonon emission, the phonon energy has to be subtracted, whereas for phonon absorption the phonon energy has to be added. For indirect transitions the density of exciton states is proportional to  $(E - E_0)^{0.5}$ .<sup>23,24</sup> The free excitons’ annihilation luminescence for Ge should therefore have the form  $(E - E_0)^{0.5} e^{-(E-E_0)/kT}$ .<sup>25</sup> In approximation

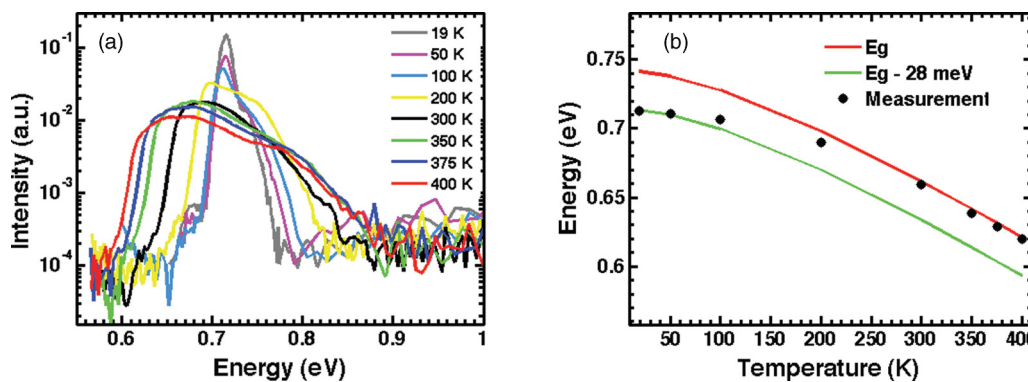


FIG. 4. (Color online) (a) Photoluminescence measurements of intrinsic Ge at different temperatures. (b) The energy of the left PL edge is plotted as a function of temperature. The band-gap energy as a function of temperature according to Ref. 12 is also shown with and without an offset of  $-28$  meV.

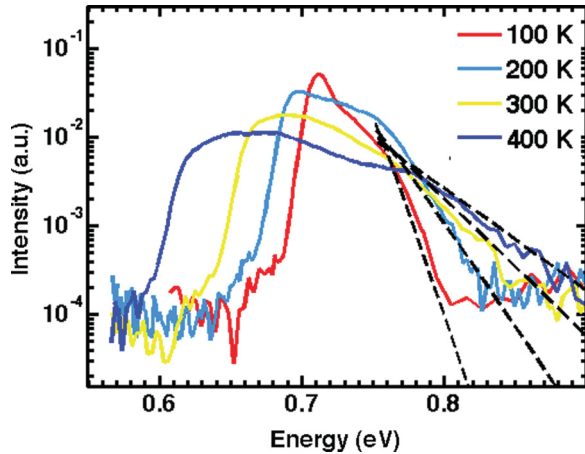


FIG. 5. (Color online) Photoluminescence measurements of intrinsic Ge at different temperatures. The right PL edge can be fitted by an exponential broadening as a function of temperature.

this behavior has been demonstrated for Ge at 4.2 K.<sup>25</sup> We demonstrate that the slope of the high-energy PL edge follows approximately this exponential broadening behavior for temperatures of 100 K and higher; see Fig. 5. To align the calculated spectrum with the measured spectrum, phonon absorption with energy of 8 meV was used. This phonon energy corresponds to the absorption of a TA phonon. TA phonons do not exist at temperatures below 100 K. The lattice temperature has been derived by fitting the high-energy PL edge with  $(E - E_0)^{0.5} e^{-(E-E_0)/kT}$ . For the spectra measured at set point temperatures of 100, 200, 300, and 400 K, the following temperatures were fitted, respectively:  $107 \pm 4$  K,  $224 \pm 3$  K,  $286 \pm 1$  K, and  $390 \pm 1$  K. Although the peak intensity decreases to 12% when the temperature increases from 19 to 300 K, the integrated intensity only decreases to 55%. This indicates that the radiative recombination in Ge is efficient at 300 K compared to low temperature.

## VI. CONCLUSIONS

A weak luminescence feature at 738 meV is observed at 7 K for Ge substrates with Al and Sb dopants, but not for intrinsic and Ga-doped Ge. This feature can be explained by no-phonon (NP)-assisted recombination of free excitons. Besides the NP feature for doped Ge, intense luminescence peaks are observed at 730, 710, and 702 meV, which can be attributed to

phonon-assisted exciton recombination of transverse acoustic (TA), longitudinal acoustic (LA) and transverse optical (TO) phonons in the (111) direction. The longitudinal optical (LO) phonon has energy close to the LA phonon in the (111) direction, and could not be resolved at 4.3 K. The presence of dopants (Al, Ga, Sb) has no significant influence on the spectral shape for dopant levels of  $(1-6) \times 10^{16} \text{ cm}^{-3}$ . Besides these features, we observe luminescence at energy below 700 meV ( $1.77 \mu\text{m}$ ). This luminescence shows much lower intensity (about 500 times) than the LA replica. The observed luminescence can be explained as a two-phonon-assisted recombination with the previously mentioned TA, LA, LO, and TO phonons with momentum in the (111) direction (at the  $L$  point) and a TO phonon at the  $\Gamma$  point. The power dependence of the integrated PL shows a log-log dependence with a power factor of 2.02 at 9 K. This indicates that the PL originates from recombination of excitons, which are indirectly generated by creation of electrons and holes. For the LA and TA phonon replica, as well as the second-order  $\text{TO}(L) + \text{TO}(\Gamma)$  phonon replica, we observe quadratic power dependence. The low-energy PL edge follows the temperature dependence of the band gap as function of temperature. The TO phonon replica determines the left edge at temperatures below 100 K. At temperatures above 100 K the left PL edge is determined by another transition with an increase in optical emission energy of 28 meV. This energy shift could be due to the dominance of the TA phonon emission, which is shifted by 28 meV in respect with the TO emission, or due to additional absorption of LA phonons at the  $L$  point. The high-energy PL edge shows an exponential broadening as a function of temperature. The position of the high-energy PL edge can be explained by TA phonon absorption above 100 K.

## ACKNOWLEDGMENTS

R.R.L. acknowledges support as Research Fellow of the Research Foundation—Flanders (FWO) and support of the Belgian American Educational Foundation (BAEF). This work was supported by the Director, Office of Science, Office of Basic Energy Sciences, Materials Sciences and Engineering Division, of the US Department of Energy under Contract No. DE-AC02-05CH11231. K.B. acknowledges support from the National Science Foundation under Contract No. DMR-0902179.

\*Corresponding author: ruben.lieten@fys.kuleuven.be

<sup>1</sup>R. F. Potter, *Handbook of Optical Constants of Solids II* (Academic, New York, 1985), p. 465.

<sup>2</sup>J. R. Jain, A. Hryciw, T. M. Baer, D. A. B. Miller, M. L. Brongersma, and R. T. Howe, *Nat. Photonics* **6**, 398 (2012).

<sup>3</sup>R. Kaufmann, G. Isella, A. Sanchez-Amores, S. Neukom, A. Neels, L. Neumann, A. Brenzikofer, A. Dommann, C. Urban, and H. Von Känel, *J. Appl. Phys.* **110**, 023107 (2011).

<sup>4</sup>S. Assefa, F. Xia, S. W. Bedell, Y. Zhang, T. Topuria, P. M. Rice, and Y. A. Vlasov, *Opt. Express* **18**, 4986 (2010).

<sup>5</sup>M. Oehme, M. Kaschel, J. Werner, O. Kirfel, M. Schmid, B. Bahouchi, E. Kasper, and J. Schulze, *J. Electrochem. Soc.* **157**, H144 (2010).

<sup>6</sup>P. K. Basu, N. R. Das, B. Mukhopadhyay, G. Sen, and M. K. Das, *Opt. Quantum Electron.* **41**, 567 (2009).

<sup>7</sup>M. Morse, O. Dosunmu, T. Yin, Y. Kang, H. D. Liu, G. Sarid, E. Ginsburg, R. Cohen, S. Litski, and M. Zadka, *Physica E* **41**, 1076 (2009).

<sup>8</sup>J. Liu, X. Sun, R. Camacho-Aguilera, L. C. Kimerling, and J. Michel, *Opt. Lett.* **35**, 679 (2010).

- <sup>9</sup>R. E. Camacho-Aguilera, Y. Cai, N. Patel, J. T. Bessette, M. Romagnoli, L. C. Kimerling, and J. Michel, *Opt. Express* **20**, 11316 (2012).
- <sup>10</sup>E. E. Haller, W. L. Hanse, G. S. Hubbard, and F. S. Goulding, *IEEE Trans. Nucl. Sci.* **23**, 81 (1976).
- <sup>11</sup>D. Poelman, O. De Gryse, N. De Roo, O. Janssens, P. Clauws, W. Bras, I. P. Dolbnya, and I. Romandic, *J. Appl. Phys.* **96**, 6164 (2004).
- <sup>12</sup>Y. P. Varshni, *Physica* **34**, 149 (1967).
- <sup>13</sup>A. Fropa, G. A. Thomas, R. E. Miller, and E. O. Kane, *Phys. Rev. Lett.* **34**, 1572 (1975).
- <sup>14</sup>G. A. Thomas, E. I. Blount, and M. Capizzi, *Phys. Rev. B* **19**, 702 (1979).
- <sup>15</sup>I. C. Cheeseman, *Proc. Phys. Soc. A* **65**, 25 (1952).
- <sup>16</sup>T. Nishino, M. Takeda, and Y. Hamakawa, *J. Phys. Soc. Jpn.* **37**, 1016 (1974).
- <sup>17</sup>W. Klingenstein and H. Schweizer, *Solid-State Electron.* **21**, 1371 (1978).
- <sup>18</sup>J. Wagner and L. Vinna, *Phys. Rev. B* **30**, 7030 (1984).
- <sup>19</sup>M. El Kurdi, H. Bertin, E. Martincic, M. de Kersauson, G. Fishman, S. Sauvage, A. Bosseboeuf, and P. Boucaud, *Appl. Phys. Lett.* **96**, 041909 (2010).
- <sup>20</sup>T. Schmidt and K. Lischka, *Phys. Rev. B* **45**, 8989 (1992).
- <sup>21</sup>D. E. Cooper, J. Bajaj, and P. R. Newman, *J. Cryst. Growth* **86**, 544 (1988).
- <sup>22</sup>H. M. van Driel, A. Elci, J. S. Bessey, and M. O. Scully, *Solid State Commun.* **20**, 837 (1976).
- <sup>23</sup>R. J. Elliott, *Phys. Rev.* **108**, 1384 (1957).
- <sup>24</sup>G. G. Macfarlane, T. P. Mclean, J. E. Quarrington, and V. Roberts, *J. Phys. Chem. Solids* **8**, 388 (1959).
- <sup>25</sup>C. Benoit à la Guillaume and M. Voos, *Solid State Commun.* **12**, 1257 (1973).